Available online at www.ijpe-online.com

International Journal of Performability Engineering

vol. 15, no. 2, February 2019, pp. 497-504
DOI: 10.23940/ijpe.19.02.p14.497504

New Method of Metal Magnetic Memory Signal Measuring and Denoising

S. J. Deng*, H. L. Chen, L. W. Tang, and W. Wang

Department of Artillery Engineering, Army Engineering University, Shijiazhuang, 050003, China

Abstract

The metal magnetic memory (MMM) technique can be effective in determining the initial damage of materials and structures in service and is partly applied in engineering. However, the real signals measured in engineering practice usually contain interference of the background magnetic field and measurement noise. For the influence of the background magnetic field, we designed a measuring probe constituted by two magnetic sensors that were arranged at different heights in the same vertical direction. Through the channel compensated method, we extracted principal features of the self-magnetic leakage field (SMLF) signal. As for the influence of measurement noise, we built the structure elements combined with the SMLF signal characteristic and investigated multi-scale morphological filtering to reduce the noise. The simulation and experiment results show that the proposed methods can not only suppress the background magnetic field and many kinds of noise but also protect the SMLF signal detail effectively.

Keywords: metal magnetic memory; self-magnetic fields; background magnetic field; measurement noise; life-off value; multi-scale morphological filter

(Submitted on October 15, 2018; Revised on November 17, 2018; Accepted on December 12, 2018)

1. Introduction

Many engineering components and structures in service are working under circumstances of high temperatures, high speed, and corrosion. It is advisable to conduct nondestructive inspections for monitor corrosion, cracks, and other defects [1]. However, the traditional non-destructive test (NDT) techniques, such as linear ultrasonic testing (UT), Eddy current testing (ET), and magnetic flux leakage testing (MT), are mainly used to detect already developed defects [2-4]. The metal magnetic memory (MMM) technique, proposed by Russian experts in the late 1990s, has become an emerging field recently due to its capability of early diagnosis and pre-warning of dangerous ferromagnetic work pieces and parts involving the characteristic of precise stress concentration [5-7].

MMM is a nondestructive testing method based on the analysis of self-magnetic leakage field (SMLF) distribution on components' surfaces for the determination of stress concentration zones, imperfections, and heterogeneity of metal structures and welded joints. Because the physical mechanism of MMM method is still unclear so far, many researchers have devoted their efforts to investigate variation regularities of MMM signals in the laboratory. Previous research on the MMM method concentrated on the variation of MMM signal under tensile stresses, cyclic tensile–compressive stress, and the magneto mechanical effect, and the physical mechanism of the metal magnetic memory phenomenon has also been discussed in rotary bending fatigue experiments [8-11]. Although several experimental studies have been carried out and many important achievements have been made, most of the research focuses on analyzing normal components of magnetic leakage fields, and little work has been done on MMM engineering signal processing.

The real signals measured in engineering practice usually contain interference noise. Since SMLF is a kind of weak magnetic field and is sensitive to noise, the background magnetic field and measurement noise have a great impact on flaw inspection. The higher the sampling frequency, the greater the influence of the same noise, so it is hardly pressed to distinguish the stress concentration zones directly. In this paper, a new detection strategy was presented to reduce the

* Corresponding author.
E-mail address: dsj_sjz@163.com

influence of background magnetic field, and multi-scale morphological filtering, a kind of nonlinear filter, was adopted to suppress various kinds of measurement noise.

2. Research on the Background Magnetic Interference Elimination

There are many kinds of magnetic testing instruments that can be used in the MMM test, and the instruments can be divided into single-channel and multi-channel according to the number of detection channels. They can also be divided into one-dimensional, two-dimensional, and three-dimensional according to the dimensions of the testing magnetic field. However, most of the magnetic testing equipment have a common characteristic: the magnetic sensors are arranged in the same horizontal plane. When detecting the surface magnetic field of the ferromagnetic specimens, the real magnetic field signal H measured in engineering practice can be expressed as

$$\boldsymbol{H} = \boldsymbol{H}_{\mathrm{p}} + \boldsymbol{H}_{\mathrm{b}} + \boldsymbol{H}_{\mathrm{z}} \tag{1}$$

Where $\boldsymbol{H}_{\mathrm{p}}$ is the magnetic field generated by the stress concentration zones (SCZs), $\boldsymbol{H}_{\mathrm{b}}$ is the background magnetic field consisting of the magnetic field caused by other equipment, the geomagnetic field, and the induced magnetic of the test specimen itself. $\boldsymbol{H}_{\mathrm{z}}$ is the measurement noise produced by the test system itself. The magnetic memory signal is not only affected by the measurement noise $\boldsymbol{H}_{\mathrm{z}}$ but also influenced by the background magnetic field $\boldsymbol{H}_{\mathrm{b}}$. The signal processing technique can only reduce the interference of $\boldsymbol{H}_{\mathrm{z}}$ because the background magnetic field $\boldsymbol{H}_{\mathrm{b}}$ cannot be known or controlled in advance. Therefore, it is hard to distinguish the SCZs directly, while the maximum magnetic field gradient value has more advantages. Because the magnetic field gradient value is obtained from the first derivation of the real signals, when $\boldsymbol{H}_{\mathrm{b}}$ changes slowly and smoothly, the influence of the background magnetic field on the magnetic field gradient can be ignored, but if $\boldsymbol{H}_{\mathrm{b}}$ changes in a complicated and volatile manner, the background magnetic will have a great impact on the SMLF distribution and gradient.

The SMLF signal is affected by the SCZ width, location, and lift-off value of sensors, but the lift-off has a much greater impact on the SMLF signal than other factors. As shown in Figure 1, the amplitude of the SMLF signal drops dramatically when the lift-off value increases within a small range; therefore, the probe should be as close to the test specimen surface as possible in engineering tests [12].

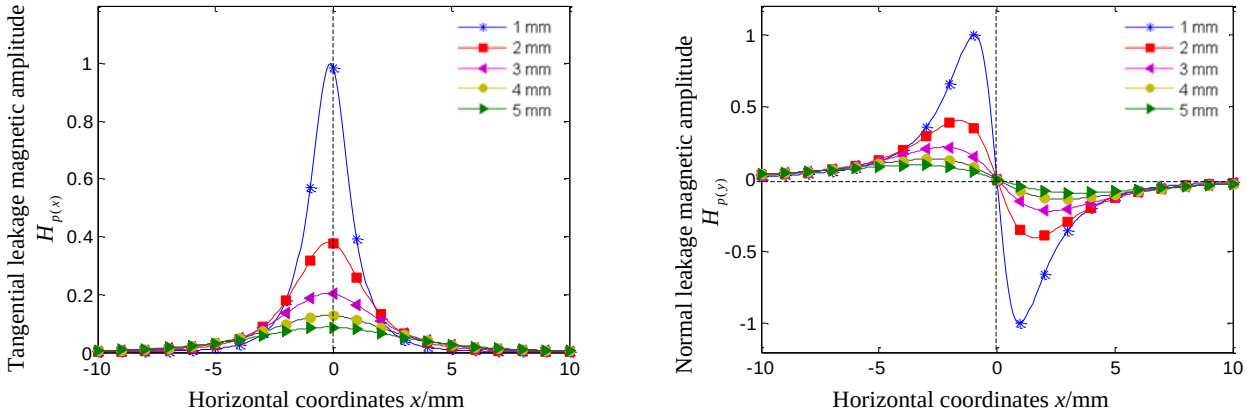

Figure 1. The effect of lift-off value on the distribution of SMLF signals

Because the lift-off has a great impact on the SMLF, a double-sensor probe is designed as shown in Figure 2.

Since the test specimen volume is much bigger than the SCZ volume and the distance from the environment magnetic field source to the probe is much longer than the distance of *D* between the two magnetic sensors, the background magnetic field signals measured by the two sensors is approximately the same while the SMLF signals has a large difference. The channel 1 test signal is the detection signal, and the channel 2 test signal is the compensation signal. The channel compensated method can eliminate the influence of the background magnetic field.

As Figure 3 shows, a specimen with an appreciable SCZ was inspected by the MMM method. The magnetic flux leakage was measured by magnetic sensor HMC5883L produced by Honeywell, and the lift-offs of the two sensors were 1mm and 4mm. The magnetic field signals were recorded along the specimen length direction line and scanned by a step of 0.2mm.

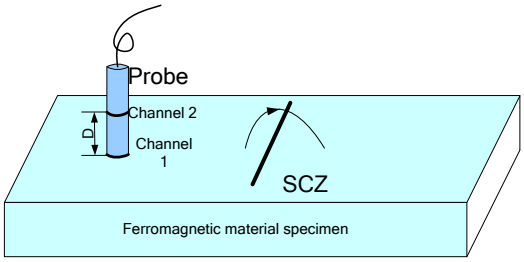

Figure 2. Schematic diagram of magnetic memory test

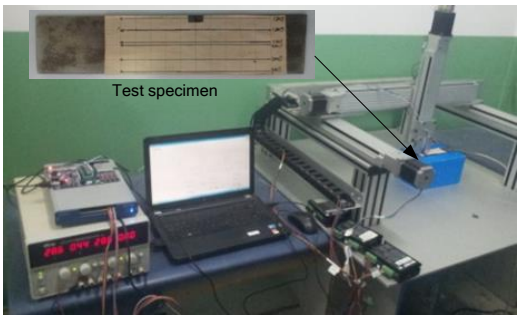

Figure 3. Photo of experiment

Figure 4 shows the detection result of a ferromagnetic specimen. The curves Ch1 and Ch2 were measured by channel 1 and channel 2 respectively, and the curve Ch1-Ch2 was the differential signal of Ch1 and Ch2. It is obvious that the differential signal removed the stable interference of the background magnetic field and protected the detail of the SMLF signal well, and it also has the advantage of anti-electromagnetic interference.

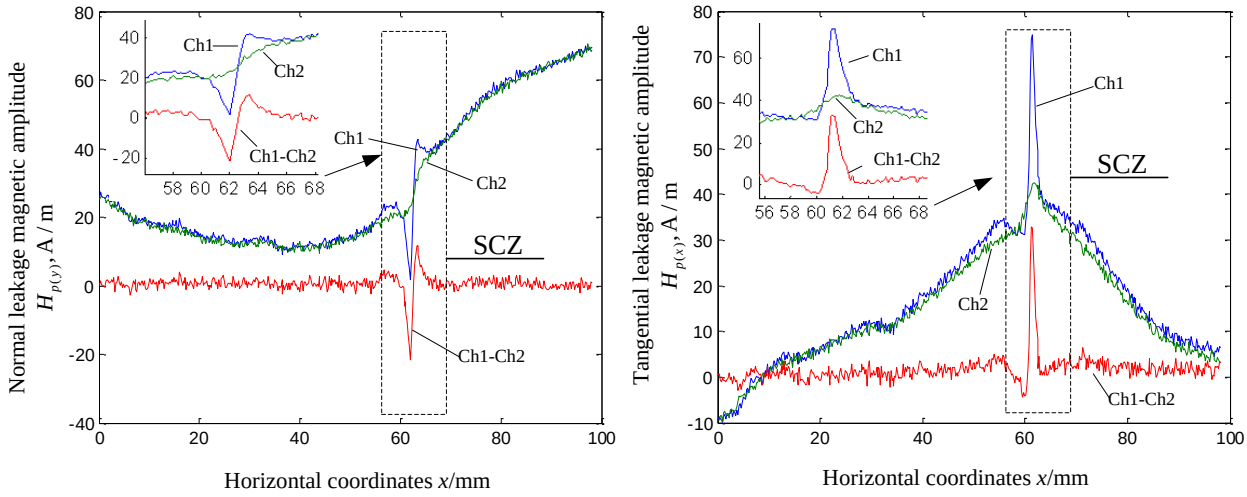

Figure 4. Detection result of metal magnetic memory

3. Research on the Measurement Noise Interference Elimination

The channel compensated method can reduce the interference of the environment magnetic field and equipment working electromagnetic, but it cannot avoid the influence of measurement noise. Because the SMLF belongs to a non-stationary signal, the application of a self-adaptive digital filtering is limited. Therefore, we try to seek a new method to reduce the measurement noise and introduce morphological filtering into SMLF signal processing. Morphological filtering is a kind of nonlinear filtering method that has good filter performance and good flexibility, and it is widely used in vision detection, noise suppressing, edge extraction, and pattern recognition. In this paper, we discuss mainly the basic theory of morphological filtering, design the structuring elements according to the characteristics of the SMLF signal, and propose a multi-scale morphology filtering for denoising.

3.1. Introduction of Morphological Filtering

There are four kinds of basic mathematical morphological transformation [13]: dilation, erosion, opening, and closing. Let $f(n)$ be a discrete real function on the one-dimensional space Z, and structure element g(m) the subset of Z. Then, dilation(Θ) and erosion($\oplus$) $f(n)$ with respect to $g(m)$ are defined as follows:

$$(f \Theta g)(n) = \min\{f(n+m) - g(m)\}, \qquad n = 0,1,\cdots, N-M \tag{2}$$

$$(f \oplus g)(n) = \max\{f(n-m) + g(m)\}, \qquad n = M-1, M, \cdots, N-1 \tag{3}$$

Morphological opening($\circ$) and closing($\bullet$) of (n) with respect to $g(m)$ are

$$(f \circ g)(n) = (f \Theta g \oplus g)(n) \tag{4}$$

$$(f \bullet g)(n) = (f \oplus g \Theta g)(n) \tag{5}$$

Morphological opening-closing and closing-opening filters are defined as follows:

$$OC(f(n)) = (f \circ g \bullet g)(n) \tag{6}$$

$$CO(f(n)) = (f \bullet g \circ g)(n) \tag{7}$$

Where OC is denoted as an opening operation followed by a closing operation and CO is denoted as a closing operation followed by an opening operation. Through the cascade connection of opening and closing, both the positive and negative noise can be eliminated using the same structure element. Moreover, to weaken the statistical deviation problem existing in open-closing and close-opening filters, the two filters are combined together to form a new filter:

$$y(n) = [OC(f(n)) + CO(f(n))]/2 \tag{8}$$

3.2. Selection of Structure Element

The selection of the structure element includes the selection of the shape, the width, and the height. According to reference [14], the selection of the structuring element has a great influence on the effect of the filtering. In order to get a good filtering effect, the structuring element should be similar to the useful signal. We propose the structuring elements in the light of tangential and normal magnetic signals of SMLF as follows:

$$g_x(m) = k \operatorname{arc\,cot}(\frac{m^2}{L}), \qquad -L < m < L,\ k \in R \tag{9}$$

$$g_y(m) = k \arctan(\frac{mL}{5(L+m^2)}), \qquad -L < m < L,\ k \in R \tag{10}$$

The shapes of the proposed structuring elements are shown in Figure 5, and we can adjust the value of L and k to control the width and height of the structuring elements.

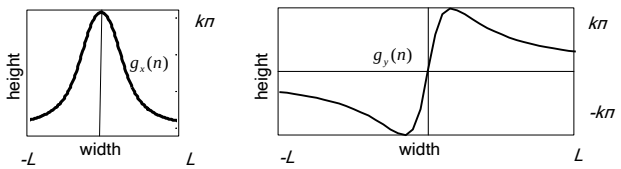

Figure 5. Shape of structure element

3.3. Multi-Scale Morphological Filter

The selection of structuring element width on the filtering effect is the most important. If the width of the structuring

element is too small, the noise cannot be removed completely. On the contrary, if the width is too large, the wanted signal will be distorted. In order to remove the noise completely and preserve the features of the SMLF signal, a multi-scale morphology filter was proposed [15]. The multi-scale morphological opening and closing are defined as

$$(f \circ g)_s(n) = (f \Theta sg) \oplus sg(n) \tag{11}$$

$$(f \bullet g)_s(n) = (f \oplus sg) \Theta sg(n) \tag{12}$$

Where *sg* is the width of structuring element *s*. The multi-scale morphology filtering algorithm is illustrated in Figure 6.

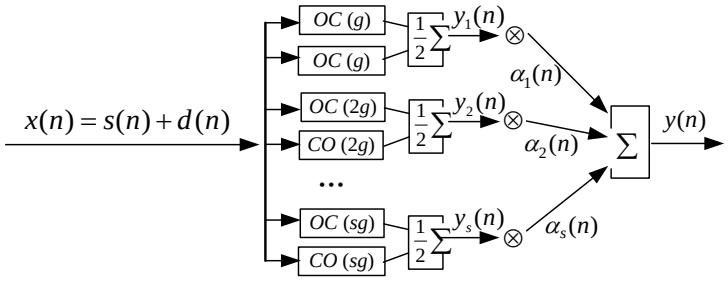

Figure 6. The diagram of the adaptive multi-scale morphological algorithm

Where $x(n)$ is the input signal, $s(n)$ is the noise-free signal, $d(n)$ is the noise signal, $y_s(n)$ is the output signal after the combined morphology filter in which the width of the structuring element is s, $\alpha_i(n)$ is the weight of $y_i(n)$, and $y(n)$ is the final output signal that can be expressed as

$$y(n) = \sum_{i=1}^{i=s} \alpha_i(n) y_i(n) \tag{13}$$

The difference between the filter output $y(n)$ and $s(n)$ is

$$e(n) = s(n) - y(n) \tag{14}$$

The mean square error is

$$E(e^2(n)) = E\left[\left(s(n) - \sum_{i=1}^{i=s} \alpha_i(n) y_i(n)\right)^2\right] \tag{15}$$

Meanwhile, there exists

$$\nabla = \frac{\partial[e^2(n)]}{\partial \alpha_i(n)} = -2y_i(n)e(n), \qquad i = 1, 2, \cdots, s \tag{16}$$

When the mean square error reaches its minimum, $\nabla = 0$. According to the gradient descent method,

$$\alpha_{i+1} = \alpha_i + 2uy_i(n)e(n), \qquad i = 1, 2, \cdots, s-1 \tag{17}$$

Where μ is the learn rate and i is the order of the filter arm. Since the noise-free signal cannot be known in practice, we can use the input signal $x(n+1)$ to replace $s(n)$.

3.4. Comparison of the Effects of Morphological Filtering with those of Conventional Filtering

In MMM testing signal processing, there are many other noise reducing methods, such as wavelet filtering and neighbor average filtering. Now, we make a comparison of the effects of morphological filtering, wavelet filtering, and neighbor

average filtering.

In this simulation experiment, the expression of noise-free signal is $y(t) = 2\sin(2\pi ft)$ (in which f = 1, t = 0 ~ 10, and the interval is 0.01), and the mixed noise signal consists of Gaussian noise, positive impulse noise, and negative impulse noise. The structuring element shape of morphological filtering used in the experiment is a straight line, and the width is 5. The wavelet basis function of wavelet filtering is db8, and the number of wavelet decompositions is 6. The window width of the neighbour average filter is 5.

Figure 7 shows the effects of removing random and impulse noise with the three kinds of filter.

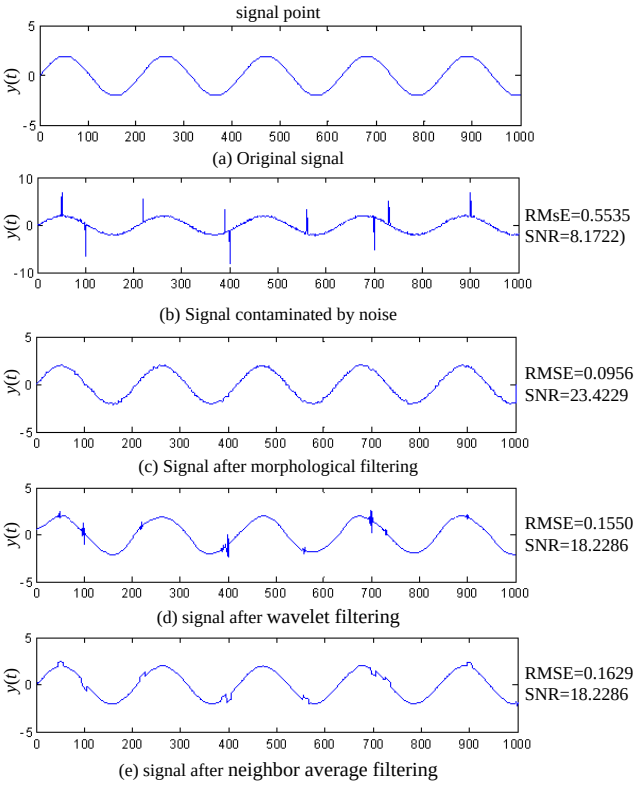

Figure 7. Comparison among the denoising results of different methods

From the shape, the root mean square error (RMSE), and signal to noise ratio (SNR), we can see that the effect of morphological filtering is better than the other two. The effects of wavelet filtering largely depend on the chosen wavelet basis function. Nevertheless, the frequency and amplitude of noise are changing and unpredictable, so it is not easy to choose a suitable wavelet basis function that is not self-adaptive. Neighbour average filtering can reduce the interference of Gaussian noise, but it cannot remove the influence of impulse noise. Morphological filtering transforms the test signal with the structuring element of a certain shape, measuring and picking up the corresponding shape in the test signal; thus, morphological filtering should not care about the characteristic of noise.

In order to ensure the suitable range value of the structuring element width, we suppress the noise filtering with different widths of the structuring element. The effects of different widths of the structuring element are shown in Figure 8.

Therefore, we should select a proper width range value based on the character of the SMLF signal. As for the SMLF signal, supposing the greatest width of the SCZs signal is T and the sample interval is T_s, the greatest width of the structuring element needs to be slightly less than T/T_s to remove the mixed noise. In this experiment, for the tangential signal of SMLF, the greatest width of the structuring element chooses 9, and for the normal signal of SMLF, the greatest width of the structuring element chooses 11. The final effects of multi-scale morphology filtering are shown in Figure 9. Since the weight coefficient was set according to the error of each filter, multi-scale morphology filtering can remove the noise completely and preserve the features of the wanted signal.

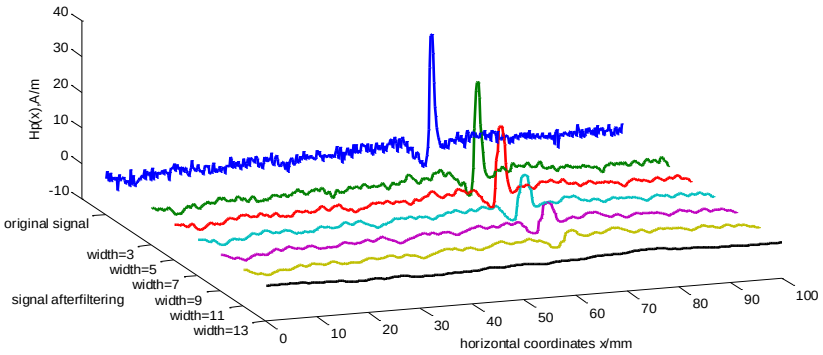

Figure 8. The morphological filtering wave by different scale length

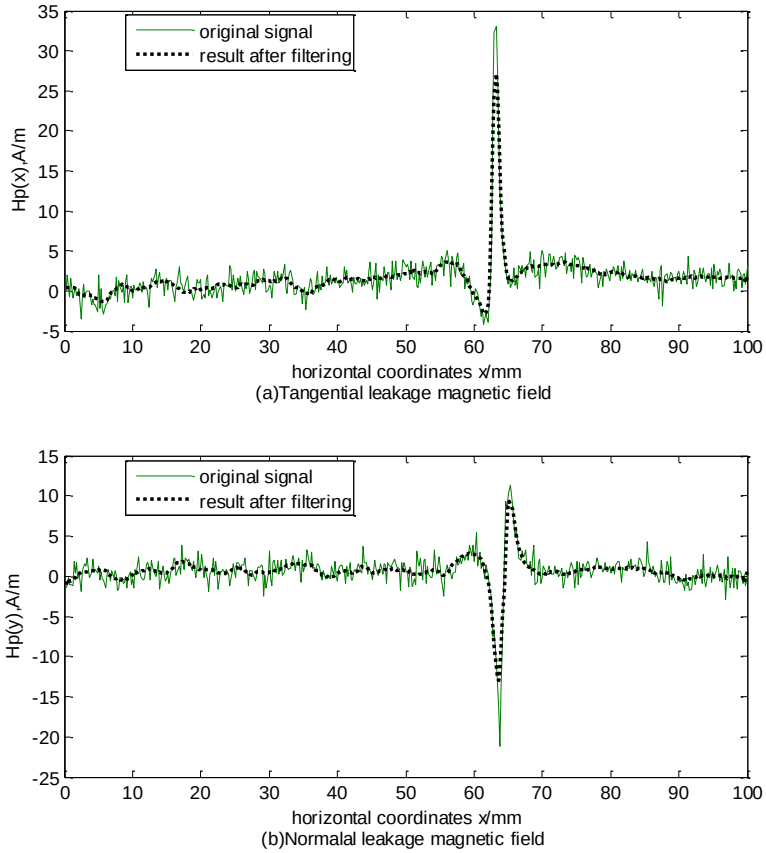

Figure 9. The signal after multi-scale morphological filtering

4. Conclusions

MMM is an effective method for early diagnosis of structural failure or fatigue damage, but the real MMM signals method always contains much inference noise. Therefore, it is necessary and important to study the method of SMLF signal extraction and noise reduction in engineering.

As a substitute for the existing SMLF measurement methods, the channel compensation program can eliminate interference by the static background magnetic field and dynamic magnetic field. It reduced the MMM method's requirements of the test environment.

The morphological filtering is totally self-adaptive and does not need manual intervention. The speed of calculation of the method is very high because the operation only involves addition and subtraction. With the structure elements built

according to the SMLF signal characteristics, multi-scale morphological filtering achieved good performance in reducing pulse noise and random noise, while preserving the feature of the SMLF signal.

We should select a proper distance between two channels. If the distance is too long, the residual magnetic of specimen attenuates and the background magnetic field cannot be separated completely. On the contrary, if the distance is too short, the wanted signal in the differential signal will be lost. The proper distance can be determined by testing; however, further work will be required to select the distance of two channels according to the detection position and volume of the specimen.

Acknowledgements

We would like to thank the reviewers for their valuable comments. This work was partially funded by the National Natural Science Foundation of China and the Military Research Foundation of China.

References

1. P. Shi, P. Zhang, and K. Jin, "Thermo-Magneto-Elastoplastic Coupling Model of Metal Magnetic Memory Testing Method for Ferromagnetic Materials," *Journal of Applied Physics*, Vol. 123, No. 14, pp. 145102, 2018
2. H. L. Chen, C. L. Wang, and X. Z. Zuo, "Research on Methods of Defect Classification based on Metal Magnetic Memory," *Ndt & E International*, Vol. 99, No. 1, pp. 82-87, 2017
3. A. Dubov, "A Study of Metal Properties using the Method of Magnetic Memory," *Metal Science & Heat Treatment*, Vol. 39, No. 9, pp. 401-405, 1997
4. A. Dubov and S. Kolokolnikov, "The Metal Magnetic Memory Method Application for Online Monitoring of Damage Development in Steel Pipes and Welded Joints Specimens," *Welding in the World*, Vol. 57, No. 1, pp. 123-136, 2013
5. S. Bao, M. Fu, and Y. Gu, "Quantitative Characterization of Stress Concentration of Low-Carbon Steel by Metal Magnetic Memory Testing," *Materials Evaluation*, Vol. 75, No. 3, pp. 397-405, 2017
6. B. Liu, Y. Y. He, and H. Zhang, "Study on Characteristics of Magnetic Memory Testing Signal based on the Stress Concentration Field," *Iet Science Measurement & Technology*, Vol. 11, No. 1, pp. 2-8, 2017
7. W. S. Singh, R. Stegemann, and M. Kreutzbruck, "Mapping of Deformation-Induced Magnetic Fields in Carbon Steels using a GMR Sensor based Metal Magnetic Memory Technique," *Journal of Nondestructive Evaluation*, Vol. 37, No. 2, pp. 21-27, 2018
8. M. B. Arkulis, M. P. Baryshnikov, and N. I. Mishenva, "On Problems of Applicability of the Metal Magnetic-Memory Method in Testing the Stressed-Deformed State of Metallic Constructions," *Russian Journal of Nondestructive Testing*, Vol. 45, No. 8, pp. 526-528, 2009
9. Y. Y. Reutov, "A Ferromagnetic Disk in a Constant Axially Symmetric Inhomogeneous Magnetic Field," *Russian Journal of Nondestructive Testing*, Vol. 51, No. 3, pp. 146-150, 2015
10. H. P. Wang, L. H. Dong, S. Y. Dong, and B. S. Xu, "Fatigue Damage Evaluation by Metal Magnetic Memory Testing," *Journal of Central South University*, Vol. 21, No. 1, pp. 65-70, DOI 10.1007/s11771-014-1916-5, 2014
11. M. X. Xu, Z. H. Chen, and M. Q. Xu, "Micro-Mechanism of Metal Magnetic Memory Signal Variation During Fatigue," *International Journal of Minerals, Metallurgy and Materials*, Vol. 21, No. 3, pp. 259-265, 2014
12. K. Yao, Z. D. Wang, and B. Deng, "Experimental Research on Metal Magnetic Memory Method," *Experimental Mechanics*, Vol. 52, No. 3, pp. 305-314, 2012
13. J. Chou, R. C. Weger, and J. M. Ligtenberg, "Segmentation of Polar Scenes using Multi-Spectral Texture Measures and Morphological Filtering," *International Journal of Remote Sensing*, Vol. 15, No. 5, pp. 1019-1036, 1994
14. Y. Li, X. Liang, and M. J. Zuo, "A New Strategy of Using a Time-Varying Structure Element for Mathematical Morphological Filtering," *Measurement*, Vol. 106, pp. 53-65, 2017
15. Y. Li, X. Liang, and J. Lin, "Train Axle Bearing Fault Detection using a Feature Selection Scheme based Multi-Scale Morphological Filter," *Mechanical Systems & Signal Processing*, Vol. 101, pp. 435-448, 2018